Experimental Observation of Magnetic Surface Polaritons in FeF_2 by Attenuated Total Reflection

M. R. F. Jensen,[1] T. J. Parker,[1] Kamsul Abraha,[1,2] and D. R. Tilley[1,3]

[1]*Department of Physics, University of Essex, Colchester CO4 3SQ, United Kingdom*
[2]*Jurusan Fisika FMIPA, Universitas Gadjah Mada, Yogyakarta 55281, Indonesia*
[3]*School of Physics, Universiti Sains Malaysia, 11800 USM Penang, Malaysia*

(Received 8 May 1995)

We present the first direct experimental evidence for the existence of magnetic surface polaritons in a uniaxial antiferromagnet. The modes are excited in FeF_2 by attenuated total reflection with the uniaxis along an applied magnetic field H_0. The resonance is observed as an attenuation of the reflected intensity as the frequency of the far-infrared beam is scanned. We find nonreciprocity between the $+H_0$ and $-H_0$ spectra as a consequence of the nonreciprocity of the surface polariton modes when H_0 is introduced. We also observe broad dips due to the excitation of bulk modes.

PACS numbers: 75.50.Ee, 75.30.Pd, 76.50.+g, 78.20.Ci

Surface polaritons are now well established as a sensitive probe in surface analysis. The study of surface plasmon polaritons, for example, provides valuable information about material parameters associated with surface plasma oscillations such as the effective masses of charge carriers and surface charge densities. This technique has been applied to studies of metals [1] and semiconductors and semiconductor superlattices [2–5].

In ferromagnets, the study of magnetostatic surface spin waves by Brillouin light scattering has yielded important information on interface exchange constants, bulk and surface anisotropies, surface magnetization, and spin-reorientation transitions for thin films and superlattices [6–9]. In contrast, the experimental study of surface modes and the surface structure of antiferromagnets has been almost completely neglected. This is despite the fact the magnetic surface structure in antiferromagnets has recently been emphasized in a number of fundamental works [10], and also has technological importance in the exchange biasing of ferromagnetic films [11].

We report the first direct experimental observation of magnetic surface polaritons on the uniaxial antiferromagnet FeF_2 by attenuated total reflection (ATR). The present development of ATR for magnetic surface excitations opens up the possibility of a wide range of experimental studies of magnetic surfaces in the far-infrared (FIR) spectral range. This technique should be applicable to studying surface modes and parameters for a wide variety of other magnetic materials. These include ferrimagnets, easy-plane antiferromagnets [12], rare earth magnets with helical orderings [13,14], and rare earth and antiferromagnetic superlattices [15].

Magnetic surface polaritons (MSPs) were theoretically discussed first for ferromagnets [16] and later for antiferromagnets [17,18]. Subsequently a large theoretical literature has appeared [15] but no direct measurements of MSP have yet been reported. The experiments are challenging because it is necessary to establish ATR with high-frequency resolution at low temperatures.

One of the key features to emerge from the theoretical studies is that MSP propagation is nonreciprocal, i.e., reversing the direction of propagation (or reversing the applied field) changes the ATR reflectively. In our experimental results we indeed find a pronounced nonreciprocal reflectively. In addition, when the applied field H_0 is turned off, the reflection becomes reciprocal as predicted. This is in contrast to ferromagnets where nonreciprocity persists even in the absence of an applied field.

The propagation of MSPs is governed by the permeability tensor $\overleftrightarrow{\mu}(\omega)$ representing the long-wavelength response of the spin system to a driving field at frequency ω. With the z axis along $\mathbf{H}_0$ and the sublattice moments parallel to $\mathbf{H}_0$, $\overleftrightarrow{\mu}$ has components [19]

$$\mu_{xx} = \mu_{yy} = 1 + 4\pi\gamma^2 H_A M_S (Y^+ + Y^-), \quad (1)$$

$$\mu_{xy} = -\mu_{yx} = i4\pi\gamma^2 H_A M_S (Y^+ - Y^-), \quad (2)$$

with $Y^{\pm} = [\omega_r^2 - (\omega \pm \gamma H_0 + i\Gamma)^2]^{-1}$, $\mu_{zz} = 1$, and all other components vanish. H_A is the anisotropy field, M_S the sublattice magnetization, γ the gyromagnetic ratio, and Γ the damping. $\omega_r = \gamma(2H_A H_E + H_A^2)^{1/2}$ is the antiferromagnetic resonance (AFMR) frequency with exchange field H_E. We consider MSPs propagating along the interface $y = 0$ between vacuum ($y < 0$) and the medium ($y > 0$) in the Voigt geometry. This leads to propagation normal to $\mathbf{H}_0$ along the x axis and parallel to the surface (x-z plane). The detailed derivation of the dispersion relation is given elsewhere [17,20]. The MSP is found to be TE or s polarized with the only nonvanishing component of electric field $\mathbf{E}$ along $\mathbf{H}_0$. The implicit dispersion relation is then

$$\mu_V \alpha_0 + \alpha - iq\mu_{xy}/\mu_{xx} = 0, \quad (3)$$

with the spatial decay constants

$$\alpha_0 = (q^2 - \omega^2/c^2)^{1/2}, \quad \alpha = (q^2 - \varepsilon\mu_V\omega^2/c^2)^{1/2}, \quad (4)$$

where $\mu_V = \mu_{xx} + \mu_{xy}^2/\mu_{xx}$ is the Voigt permeability, ε the dielectric constant of the crystal, and $q = |\mathbf{q}|$

 0031-9007/95/75(20)/3756(4)$06.00

the magnitude of the mode wave vector. The linear term $q\mu_{xy}/\mu_{xx}$ in (3) implies nonreciprocal propagation of the surface mode. That is, changing the sign of q will change the frequency ω: $\omega(-q) \neq \omega(q)$. More generally, the sign of μ_{xy} changes under field reversal and equivalently this changes the sign of q as seen in (3), so that $\omega(q, -H_0) = \omega(-q, H_0) \neq \omega(q, H_0)$. In zero field, however, $\mu_{xy} = 0$ and q appears only as even powers so that propagation is reciprocal. The dispersion relation for the magnetic bulk polariton (MBP) is $q^2 = \varepsilon\mu_V\omega^2/c^2$, which is also even in q so the bulk-mode propagation is reciprocal.

In Fig. 1 we plot dispersion curves for FeF_2 obtained from (3), using the experimental parameters from oblique-incidence reflectivity measurements [21,22]: $H_E = 53.3$ T, $H_A = 19.7$ T, and $M_S = 560$ G. With $\gamma = 1.05\ \mathrm{cm}^{-1}/\mathrm{T}$, the AFMR frequency is $\omega_r = 52.45\ \mathrm{cm}^{-1}$ or 1.57 THz. In order to show real ω versus real q, we plot the curves without damping. For $H_0 = 0$, Fig. 1(a), the MSP starts at the intersection between the top of lower bulk band and the vacuum light line. As $|q| \to \infty$, the curves approach the magnetostatic frequency $\omega_S = (\omega_r^2 + 4\pi\gamma^2 H_A M_S)^{1/2}$. Both bulk and surface modes are clearly reciprocal in q. We also plot the ATR scan lines explained in the caption of Fig. 1. ATR dips are predicted when the scan lines cross the MSP curves at frequency ω_{sp}. With $H_0 = \pm 3$ T, Fig. 1(b), the bulk and surface mode curves alter radically due to Zeeman splitting. Using (1) and (2) we find that μ_V has two zeros and two poles. Because of the presence of these poles, denoted as ω_- and ω_+ three bulk polariton bands ($\mu_V > 0$) emerge. In the frequency gap ($\mu_V < 0$) between these bands we may find surface polaritons. Unlike for MnF_2 in the same geometry [17], we find four surface polariton curves for FeF_2 [18]. Two of these start at finite values of $|q|$ on the lower and upper bulk-continuum boundaries and approach the surface magnetostatic-mode frequencies $\omega_S^{\pm} = \omega_S \mp \gamma H_0$ for large $|q|$. The other two terminate at the high-frequency end at a finite value of $|q|$ and therefore have no magnetostatic counterparts. Conventionally, these are called virtual modes. In all cases, the surface modes are markedly nonreciprocal. We also plot ATR scan lines as in Fig. 1(a). ATR dips are predicted at frequencies ω_{sp}^{+} for $+H_0$ and ω_{sp}^{-} for $-H_0$ as indicated in Fig. 1(b).

In ATR, incident light of frequency ω is incident in a transparent prism at an angle $\phi > \phi_c$ with $\phi_c = \sin^{-1}(\varepsilon_p^{-1/2})$ the critical angle for total internal reflection. The incident light generates an evanescent wave in the gap below the prism with the in-plane wave vector $k_{\|} = (\omega/c)\varepsilon_p^{1/2}\sin\phi$. If the wave vector and frequency of this wave match those of the surface mode coupling occurs and power from the evanescent wave excites the surface mode. A reduction in the ATR reflectivity occurs at the mode frequency. The calculation is given elsewhere [20,23].

A purpose-built FIR Fourier transform spectrometer [24] with a nominal resolution of 0.01 cm^{-1} was used, and the FeF_2 single crystal was grown at Bell Laboratories [25]. The sample, held between the poles of a 7 T magnet with the field vertical, is spring loaded against the base of a silicon prism polished to a 0.25 μm finish and flat to $\sim$1 μm. The desired gap d is set approximately using spacers made form copper foil or single strands of

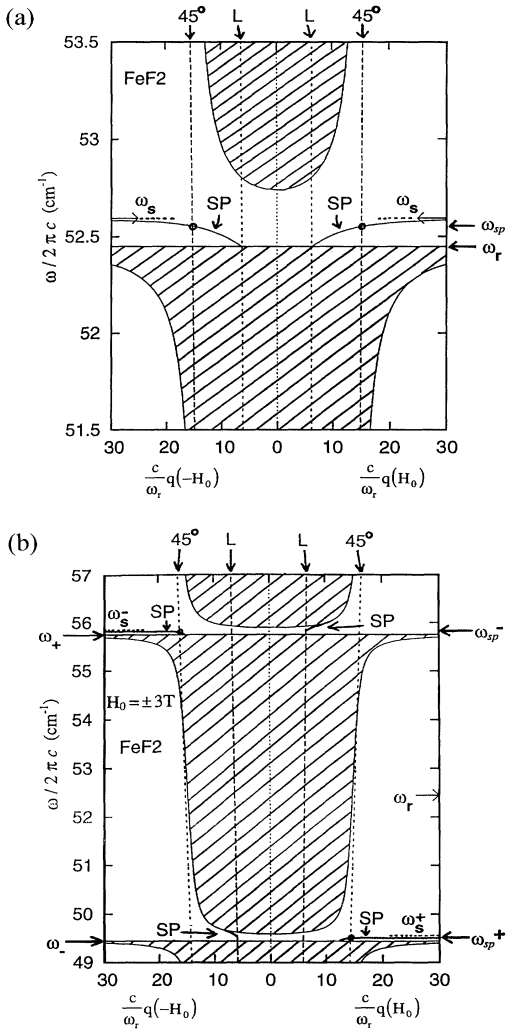

FIG. 1. Computed dispersion curves for bulk (shaded regions) and surface s-polarized (solid lines) magnetic polaritons on FeF_2. Damping is neglected and the applied field is (a) $H_0 = 0$, (b) $H_0 = \pm 3$ T. The magnetostatic frequency limits of the surface polaritons are ω_S in (a) and ω_S^{+} and ω_S^{-} in (b). In (b), ω_+ and ω_- are the pole frequencies of the Voigt permeability. Label L indicates the vacuum light line, and the ATR scan line is specified by $q = \pm\varepsilon_p^{1/2}(\omega/c)\sin\phi$ with $\varepsilon_p = 11.56$ (Si) and $\phi = 45°$. Frequencies at which the ATR scan line crosses the surface polariton dispersion curve are denoted by ω_{sp} in (a) and $\omega_{\mathrm{sp}}^{\pm}$ in (b). Note that in (b) the gaps between the bulk and surface polaritons have been exaggerated as they would not be observed on the current scale.

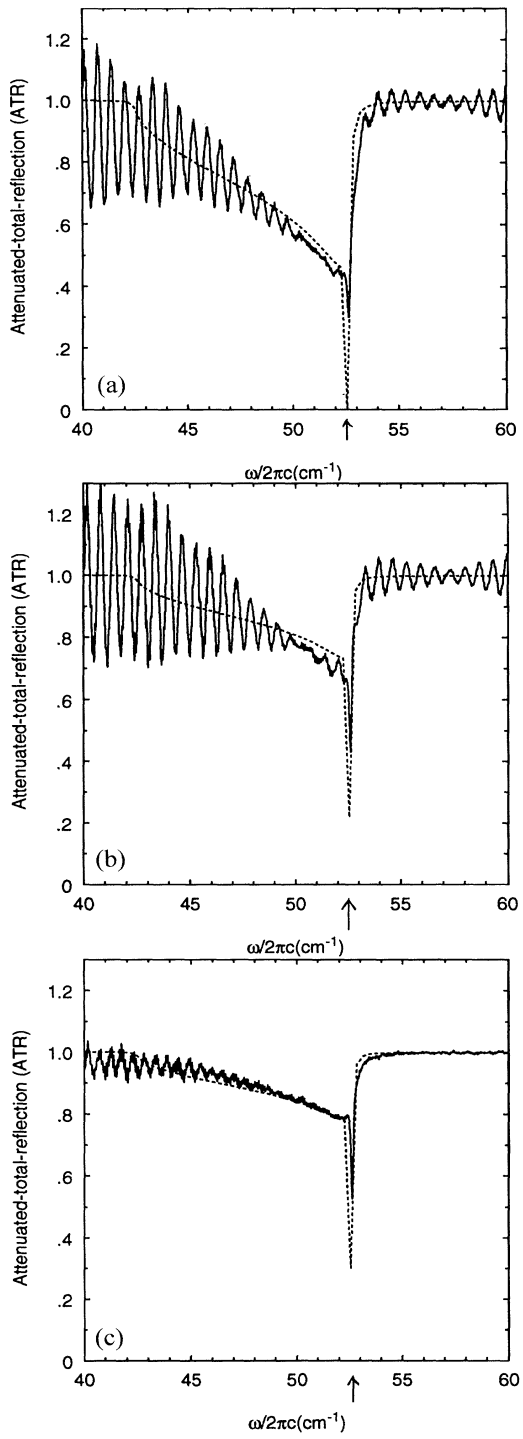

FIG. 2. Experimental (solid lines) and theoretical (dotted lines) s-polarization ATR spectra of FeF_2 at 1.6 K for $\phi = 45°$, $H_0 = 0$ and gap thickness (a) $d = 10$ μm, (b) $d = 16.5$ μm, and (c) $d = 18$ μm. Experimental resolution: 0.06 cm^{-1}. The linewidths are instrumental. Theoretical curves were drawn with $\varepsilon = 5.6$, $\varepsilon_p = 11.56$, $\omega_r = 52.45$ cm^{-1}, and damping $\Gamma = 0.05$ cm^{-1}, as quoted in Ref. [21]. The arrow indicates the surface polariton frequency ω_{sp}.

tungsten wire. A more accurate value of d is determined by a best fit of the calculated to the measured spectra.

In Fig. 2 we present theoretical and experimental ATR spectra in zero field at an angle of incidence $\phi = 45°$ in a Si prism and $T = 1.6$ K. To display the effect of varying d, three spectra were taken with $d = 10$, 16.5, and 18 μm. As d increases the ATR dip is sharpened and its depth slightly reduced, ruling out the appearance of broad dips due to MBPs. We plot the theoretical curves with $\varepsilon = 5.6$, slightly different from Ref. [21], since it is not yet clear what the correct value of ε is for FeF_2 [26]. The experimental spectra are complicated by interference fringes caused by multiple reflections between parallel surfaces of optical components, namely, the sides of the prism and the cryostat windows. Since the prism replacement accuracy (estimated to be about 200 μm) between the background (prism only) and specimen measurements is insufficient, the fringes are not removed. Another consequence is an uncertainty of up to about 20% in the overall level of the reflectively. To compensate, each experimental spectrum has been normalized by multiplying each point in the spectrum by an appropriate constant factor between 0.8 and 1.2 in order to bring the center line of the fringes close to unity in the region ~60–70 cm^{-1}.

Figure 3 shows theoretical and experimental spectra in fields of ± 3 T, $\phi = 45°$, and $d = 16.5$ μm. The spectra can be understood by reference to the ATR scan lines, Fig. 1(b). In the low-frequency region ($\omega \leq \omega_-$) the scan lines fall in the lower bulk continuum where the incident light can generate bulk polaritons and therefore the reflectivity $R < 1$ for both $H_0 = +3$ and -3 T. This is clearly seen as broad dips. All scan lines then pass through gaps between the bulk continua where no coupling to bulk polaritons occurs so that $R \rightarrow 1$. We see very sharp ATR dips with linewidths of <0.1 cm^{-1} at frequencies where the scan lines cross the MSP dispersion curves. In the high-frequency region ($\omega > \omega_+$) all the scan lines finally enter *reststrahl* regions with $R \rightarrow 1$. Small broad dips in both spectra correspond the MBP excitations as the scan lines cross parts of the bulk continua near ω_- and ω_+. The ± 3 T spectra are clearly different so Fig. 3 gives very clean and striking evidence of nonreciprocity. The MBP nonreciprocity was first reported by Remer *et al.* [27].

In this Letter we have presented experimental ATR spectra of FeF_2, which, for the first time, give clear direct evidence of the nonreciprocal propagation of MSPs in uniaxial antiferromagnets. Theoretical spectra were drawn with the same magnetic parameters obtained in oblique-incidence reflection experiments [21,22]. The overall features of both experimental and theoretical results are in very good agreement. The predicted nonreciprocity [17,18,28] is markedly displayed in Fig. 3 for $H_0 = \pm 3$ T. These results establish ATR as a powerful technique for the experimental studies of MSPs in magnetic materials where a large amount of theoretical work has been done [15,20].

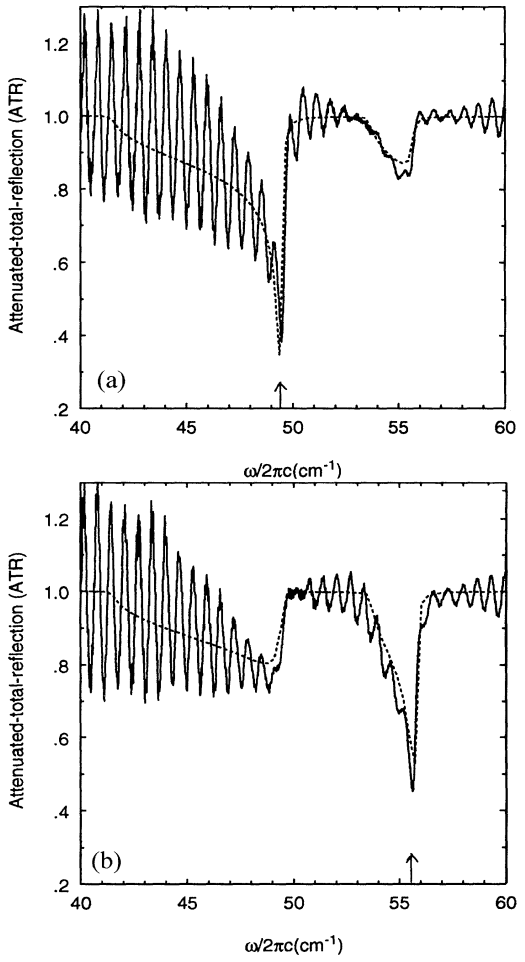

FIG. 3. Experimental (solid lines) and theoretical (dotted lines) s-polarization ATR spectra of FeF_2 with (a) $H_0 = +3$ T and (b) $H_0 = -3$ T. Experimental resolution: 0.06 cm^{-1}, fitting parameters as for Fig. 2 with $d = 16.5$ μm. The surface polariton frequencies ω_{sp}^{+} and ω_{sp}^{-} are indicated by the arrows in (a) and (b), respectively.

We now plan to carry out studies on such materials with resonances accessible to our instrument.

Helpful discussions with Doug Brown, Tom Dumelow, Stephen Smith, and Bob Camley are greatly appreciated and so is the high quality work by Glen Doel and Tony Jordan in making the prism and the sample holder. K. A. is supported by Proyek PS2PT DIKTI DEPDIKBUD (Bank Dunia XXI) Indonesia and M. R. F. J. by EPSRC. This work is part of a general program for FIR investigations of magnetic systems supported by EPSRC through Grants No. GR/G54139 and No. GR/J90831.

[1] H. Raether, *Surface Plasmons*, Springer Tracts in Modern Physics Vol. 111 (Springer, Berlin, 1988).
[2] *Surface Polaritons,* edited by V. M. Agranovich and D. L. Mills (North-Holland, Amsterdam, 1982).
[3] J. Lagois and B. Fischer, Phys. Rev. Lett. **36**, 680 (1976).
[4] F. Yang, J. R. Sambles, and G. W. Bradberry, Phys. Rev. Lett. **64**, 559 (1990).
[5] T. Dumelow, T. J. Parker, S. R. P. Smith, and D. R. Tilley, Surf. Sci. Rep. **17**, 151 (1993).
[6] P. Grünberg, in *Light Scattering in Solids,* edited by M. Cardona and G. Güntherodt (Springer, Berlin, 1989).
[7] B. Hillebrands and G. Güntherodt, in *Ultrathin Magnetic Structures II,* edited by J. A. C. Bland and B. Heinrich (Springer, Berlin, 1993).
[8] M. G. Cottam and D. J. Lockwood, *Light Scattering in Magnetic Solids* (John Wiley, New York, 1986).
[9] S. Demokritov and E. Tsymbal, J. Phys. Condens. Matter **6**, 7145 (1994).
[10] E. E. Fullerton, K. T. Riggs, C. H. Sowers, and S. D. Bader, Phys. Rev. Lett. **75**, 330 (1995).
[11] O. Allegranza and Mao-Min Chen, J. Appl. Phys. **73**, 6218 (1993).
[12] Kamsul Abraha and D. R. Tilley, J. Phys. Condens. Matter **7**, 2717 (1995).
[13] N. S. Almeida and D. R. Tilley, Phys. Rev. B **43**, 11 145 (1991).
[14] Kamsul Abraha and D. R. Tilley, Infrared Phys. Technol. **35**, 681 (1994).
[15] D. R. Tilley, in *Linear and Nonlinear Spin Waves in Magnetic Films and Superlattices,* edited by M. G. Cottam (World Scientific, Singapore, 1994), Chap. 4, and references therein.
[16] A. Hartstein, E. Burstein, A. A. Maradudin, R. Brewster, and R. F. Wallis, J. Phys. C **6**, 1266 (1973).
[17] R. E. Camley and D. L. Mills, Phys. Rev. B **26**, 1280 (1982).
[18] C. Shu and A. Caillé, Solid State Commun. **42**, 233 (1982).
[19] D. L. Mills and E. Burstein, Rep. Prog. Phys. **37**, 817 (1974).
[20] M. G. Cottam and D. R. Tilley, *Introduction to Surface and Superlattice Excitations* (Cambridge University Press, Cambridge, 1989).
[21] D. E. Brown, T. Dumelow, T. J. Parker, Kamsul Abraha, and D. R. Tilley, Phys. Rev. B **49**, 12 266 (1994).
[22] Kamsul Abraha, D. E. Brown, T. Dumelow, T. J. Parker, and D. R. Tilley, Phys. Rev. B **50**, 6808 (1994).
[23] N. S. Almeida and D. R. Tilley, Solid State Commun. **73**, 23 (1990).
[24] T. Dumelow, D. E. Brown, and T. J. Parker, in *18th International Conference on Infrared and Millimeter Waves, Colshester, 1993,* edited by James R. Birch and Terence J. Parker, SPIE Conf. Proc. No. 2104, (SPIE-International Society for Optical Engineering, Bellingham, WA, 1993), p. 633.
[25] J. Ariai, P. A. Bates, M. G. Cottam, and S. R. P. Smith, J. Phys. C **15**, 2767 (1982).
[26] R. L. Stamps, B. L. Johnson, and R. E. Camley, Phys. Rev. B **43**, 3626 (1991).
[27] L. Remer, B. Lüthi, H. Sauer, R. Geick, and R. E. Camley, Phys. Rev. Lett. **56**, 2752 (1986).
[28] R. E. Camley, Surf. Sci. Rep. **7**, 103 (1987).